Pharmaceutical Research, Vol. 25, No. 1, January 2008 (© 2007)
DOI: 10.1007/s11095-007-9509-8

Research Paper

Evaluation of Mucosal Damage and Recovery in the Gastrointestinal Tract of Rats by a Penetration Enhancer

Yogeeta Narkar,[1,5] Ronald Burnette,[2] Reiner Bleher,[3] Ralph Albrecht,[2,3,4] Angki Kandela,[3] and Joseph R. Robinson[2]

Received May 13, 2007; accepted August 15, 2007; published online December 27, 2007

Purpose. To evaluate absorption barrier recovery in the gastrointestinal tract after treatment with a penetration enhancer by using a poorly absorbed marker and correlate results with morphological recovery.
Methods. Oral gavage of sodium dodecyl sulfate (SDS) was given to Wistar rats. Phenol red (PR) was given at different time points following administration of SDS. Blood samples were obtained from the jugular vein. Pharmacokinetic analysis was performed on the *in vivo* data using WinNonlin and MATLAB®5 software. The pharmacokinetic parameters of PR were compared to the negative control to measure functional recovery. The intestinal tissues were observed using light and transmission electron microscopy.
Results. Absorption was highest when PR was co-administered with SDS. C_{max}, AUC and K_a decreased and T_{max} and MAT increased as the recovery period (time between administration of SDS and PR) increased. The pharmacokinetic parameters approached the negative control profile in one hour after treatment with 1% SDS. Microscopy results showed recovery of paracellular and transcellular barrier at this time.
Conclusions. Absorption barrier recovery could be measured using a poorly absorbed marker. Functional recovery showed a good correlation with morphological recovery. The local effects of SDS were found to be temporary and reversible.

KEY WORDS: absorption enhancement; mucosal damage; mucosal recovery; oral absorption; penetration enhancers.

INTRODUCTION

Improving oral absorption of drugs with poor oral bioavailability has always been a major focus in drug delivery research. Oral absorption of drugs can be improved by modifying the properties of drugs or by incorporating drugs into suitable vehicles. In cases where these approaches are not feasible, an alternative is to modify the barrier properties of the mucosa using penetration enhancers. Penetration enhancers have been studied for almost five decades to improve oral drug absorption. Two important aspects of these studies have been the evaluation of efficacy and safety. Efficacy of penetration enhancers in causing drug absorption enhancement has been well established by many authors. But, safety has always been a concern. The possibility of increasing absorption of toxic substances especially the endogenous endotoxins due to the local action of penetration enhancers has deterred the regulatory bodies from approving them for human use.

Under normal circumstances, the gastrointestinal mucosa forms a barrier between the body and the luminal environment (1). The gastrointestinal barrier has two components: the intrinsic barrier, which is composed of a continually renewing sheet of epithelial cells with their tight junctions (2–7) and the extrinsic barrier, which consists of mucus, bicarbonate, prostaglandins, growth factors, trefoil proteins and immunoglobulins (8–22).

Several studies have shown that the gastrointestinal barrier is occasionally ruptured by normal food materials and drugs. Examples of these materials include spices such as pepper (23,24) and garlic (25,26), hydrolytic food products and fatty meals (27,28), and alcoholic beverages (29,30). Drugs like NSAIDs (31,32), common laxatives (33–35) which are used commonly on a recurring basis and chenodeoxycholic acid (36–38) which has been used therapeutically

Electronic supplementary material The online version of this article (doi:10.1007/s11095-007-9509-8) contains supplementary material, which is available to authorized users.

Dr. Joseph R. Robinson has passed away.

[1] Product Development, Actavis, 10065 Red Run Blvd, Owings Mills, Maryland 21117, USA.
[2] School of Pharmacy, University of Wisconsin-Madison, 777 Highland Ave., Madison, Wisconsin 53705, USA.
[3] Animal Sciences, University of Wisconsin-Madison, 1675 Observatory Dr Madison, Wisconsin 53706, USA.
[4] Pediatrics, University of Wisconsin-Madison, 600 Highland Ave., Madison, Wisconsin 53705, USA.
[5] To whom correspondence should be addressed. (e-mail: ynarkar@actavis.com)

since the early 1970's for the dissolution of gallstones for up to 2 years, have been shown to cause reversible damage in the gastrointestinal mucosa (39).

This raises the following question: Is it possible to use penetration enhancers to increase oral absorption of drugs such that, after temporary alteration, absorption barrier properties of the mucosa are reestablished after the normal repair mechanisms? The main hurdle in putting this approach into practice is the lack of a quantitative method to measure barrier disruption coupled with subsequent recovery. If such a method were available, it would be possible to determine the amount of penetration enhancers that can be effectively used to increase drug permeation with a relatively quick recovery.

Measurement of damage and subsequent recovery is an integral part of any study involving penetration enhancers. Recovery is an important aspect, since this would decide if the penetration enhancer approach is practically feasible. Use of a whole, live animal model would give a better estimate of recovery due to the presence of intact blood supply and the basal lamina, as opposed to the *in vitro* systems and the lack of any external artifacts, which exist in *in situ* models.

For *in vivo* models the commonly employed methodology is histological evaluation. Histological evaluation is an important tool because it gives visual evidence of changes in morphology. However, it remains a semi-quantitative technique. Since absorption enhancers act by altering the barrier properties of the membrane, we propose to use the absorption of a marker molecule through damaged and recovered gut to obtain a more quantitative and dynamic measure of mucosal recovery. The specific aims of this study are as follows: (1) measuring kinetics of functional recovery through absorption of markers across the mucosa, during various stages of recovery, after treatment with a penetration enhancer in an intact animal. (2) Correlating functional recovery (absorption barrier recovery) with morphological recovery evaluated using microscopy techniques.

MATERIALS AND METHODS

Selection of Marker and Penetration Enhancer

The marker (phenol red) chosen is a water-soluble molecule to exclude the possibility of increased oral absorption of otherwise hydrophobic markers due to increased solubilization in the presence of penetration enhancers. Phenol red is a poorly absorbed marker, commonly employed in oral absorption studies (40–43).

The criteria for selection of a surfactant were based on known local toxicity and non-systemic toxicity. Sodium dodecyl sulfate (SDS) is an anionic surfactant. It extracts epithelial membrane components due to its surface-active behavior and disrupts paracellular junctions (44–46). In a 90-day feeding study, when rats were given 1,000 ppm of SDS in their daily diet (average consumption of 20 mg of SDS per day), it was shown to be systemically nontoxic (47). In a similar study by Fitzhugh *et al.*, 1% SDS was shown to cause no systemic toxicity when administered via diet to rats for two years (48). This was important information since it was crucial to eliminate any interference from systemic toxicity of a penetration enhancer and to ensure that the changes seen upon treatment with SDS would result solely from the local action of SDS on the intestinal mucosa. Based on the reported information (44–48), 1% SDS (34 mM) concentration was chosen as the treatment and 1.5 and 2% SDS (51 and 68 mM respectively) concentrations were used as positive controls.

Materials

All chemicals used were ACS grade and purchased from Sigma Chemicals, St. Louis, MO, unless stated otherwise. Acetonitrile and trichloroacetic acid were obtained from Fisher Scientific, St. Louis, MO. Isoflurane (IsoFlo®) was ordered from Abbott labs, Chicago, IL. Two milliliters EDTA blood collection tubes containing 50 mM of EDTA were purchased from Midwest-Vet Supply, Madison, WI. Epon resin kit (Embed 812) was ordered from EMS, Hartfield, PA. 400-mesh Nickel grids were purchased from Ted Pella, California.

Animals

Male Wistar albino rats (weighing about 300 g) were used in all the experiments. The rats were obtained from Harlan, Madison, WI. The animals were housed in a temperature and humidity controlled room and were given standard rat chow and water which were freely available. All the procedures used in this study were approved by the research animal resources center (RARC), UW and adhered to the "Principles of Laboratory Animal Care" (NIH publication no. 85–23, 1985). The animals were fasted overnight with free access to water before experiments, to eliminate the effect of food on mucosal damage and recovery. At the end of the oral absorption experiments, rats were euthanized in a carbon dioxide chamber. For all morphological experiments, rats were anesthetized using isoflurane during tissue collection and euthanized by excision of the heart afterwards.

Assay of Phenol Red

Plasma proteins were precipitated by adding 20% trichloroacetic acid and acetonitrile in a 2:1:1 proportion to plasma samples. The samples were centrifuged and the supernatant solutions were assayed by reverse phase HPLC (Varian Prostar, model 210) coupled with a UV detector (Varian Prostar, model 320) set at 430 nm, on a C18 column (Econosil C18, Alltech, IL) using pH 4.0 phosphate buffer (50 mM) and acetonitrile (77:23) as a mobile phase.

Absorption Enhancement of Phenol Red with SDS

An oral gavage of phenol red (6 mg in 2 ml) with SDS (1, 1.5 or 2% *w/v*) was administered to rats using a 3.5 in. intragastric feeding tube. One percent SDS was used as the treatment and 1.5% and 2% SDS were used as positive controls. The negative control group received an oral gavage of phenol red without SDS. Blood samples were drawn from the jugular vein at 0, 10, 20, 30, 60, 120, 180 and 300 min and assayed as described above.

To evaluate pharmacokinetic parameters of phenol red, an intravenous (IV) bolus study was performed in which phenol red solution (0.25 mg in 0.1 ml) was administered into the jugular catheter and blood samples were drawn at 0, 5, 10,

15, 20, 30, 60, 90, 120, 180 and 240 min. Statistical moment analysis and two-compartment analysis were performed on the *in vivo* data using WinNonlin and MATLAB® 5 respectively.

Recovery of Absorption Barrier

Rats were given an oral gavage of 2 ml of 1% SDS. After a specific recovery time that was assigned to each group of animals i.e. 15 min, 30 min, 1 h and 3 h, rats received an oral dose of phenol red (6 mg in 2 ml). After administration of the marker, blood samples were drawn and assayed as described before. Pharmacokinetic parameters were estimated for recovery groups and compared with those of the control group (no prior exposure to SDS). For positive control, 3-h recovery experiments were performed for 1.5% and 2% SDS. Statistical moment analysis and two-compartment analysis were performed on oral absorption data for phenol red using WinNonlin and MATLAB® 5 respectively.

Recovery of Morphology

Three rats were used per group. The negative control group was given an oral gavage of water. The treatment groups were given an oral dose of 2 ml of 1% SDS. At the specific recovery time assigned to each group (10 min, 15 min, 30 min, 1 h or 3 h), rats were anesthetized with isoflurane. One cm of the duodenum was collected immediately below the pyloric sphincter. Similarly, 1 cm of the jejunum 10 cm from the pyloric sphincter was collected. The tissues were immediately washed with cold PBS (pH 7.0) and fixed with the 2.5% glutaraldehyde fixative solution in 0.1% cacodylate buffer (pH 7.0). The samples were post fixed with 1% osmium tetroxide in 0.1 M cacodylate buffer. The tissues were dehydrated in ethanol and embedded in EPON resin. The resin was then allowed to polymerize at 65°C for 48 h. Two-micrometer sections were serially cut from the resin blocks using an ultramicrotome (RMC, Arizona), stained with 1% toluidine blue solution and viewed under a light microscope (Zeiss Axiovert 200 M). For transmission electron microscopy (TEM), 100 nm sections were mounted on 400-mesh grids, contrasted with 1% lead citrate solution for 20 s and with 2% uranyl acetate in water for 10 min. The sections were observed under a transmission electron microscope (Zeiss EFTEM 912).

Pharmacokinetic and Statistical Analysis

The area under the plasma concentration-time curve from time zero to t ($AUC_{0–300\ min}$) for each treatment was calculated using the linear trapezoidal rule. The reported peak concentrations (C_{max}) and time of peak concentration (T_{max}) were obtained from the respective plasma concentration–time plots. Statistical moment (non-compartment) analysis was performed on the phenol red IV bolus and oral absorption data using WinNonlin 4.1 software (Pharsight Corporation, 1998–2003) to evaluate mean residence time (MRT) and mean absorption time (MAT) for the control and treatment groups.

Two-compartment pharmacokinetic analysis was performed on IV bolus and negative control oral absorption data for phenol red using WinNonlin 4.1 software (Pharsight Corporation, 1998–2003) to estimate distribution rate constants (K_{23}, K_{32}), elimination rate constant (K_e), volume of distribution (V_2) and absorption rate constant (K_a).

Two-compartment analysis on oral absorption of phenol red when co-administered with SDS and during recovery periods was performed using MATLAB® 5 software, since the software enabled pharmacokinetic modeling with a facility of changing K_a with time. The program used is available online as Appendix A. In this program, baseline absorption rate constant (K_{a0}) is absorption rate constant for phenol red in the negative control group. K_a is the absorption rate constant at a particular time point that gives the best model fit. Thus, when the absorption barrier is altered using a penetration enhancer, K_a is larger than K_{a0}. As the absorption barrier recovers K_a reduces and becomes equal to K_{a0} paralleling the recovery of the absorption barrier. The microconstants (K_{23}, K_{32}, K_e and V_2) and bioavailability (F) used for phenol red in these programs are the same as those determined from IV and control oral absorption studies using WinNonlin software. With MATLAB®5, the oral absorption data was modeled by using differential equations, which describe a two-compartment pharmacokinetic model with a first order absorption phase. The absorption rate constant, K_a was changed with time in a step-wise manner (step-function analysis). These values were manually selected and the predicted plasma concentrations from these selected K_a values were evaluated by goodness-of-fit statistics. In goodness-of-fit statistics, the R^2 values were calculated from the ratio of the sum of squares about the predicted plasma concentrations to the sum of squared residuals. The optimum values of K_a were obtained through repeated iterations.

The K_a values in the step-function analysis described above were initially selected manually through use of a series of decreasing step functions of variable duration. To validate these values, a continuous-function analysis was performed. Based on the results obtained from the step function analysis, a two parameter exponential function was chosen to obtain a best fit continuous time dependent K_a function for the 1% SDS, 1.5% SDS and 2% SDS treatments (continuous-function analysis). The best fit for the two parameter fit of K_a was obtained by doing a grid search for each of the parameters with the goodness-of-fit evaluation accomplished through the minimization of the sum of the squares of the differences between the predicted and observed concentration values. The MATLAB program used is given online in Appendix B. An exponential fitting function was chosen because relative to other possible functional dependencies, it allowed for the best correct initial, intermediate and final K_a values to be obtained.

The statistical program Sigmastat (Windows version 3.11, 2004, Systat software, Inc.) was used to analyze the pharmacokinetic data. Parameters obtained for the treatment groups were compared with the respective parameters from the control group using one-way ANOVA at 5% significance level. To determine the number of animals to be included in treatment and control groups, power analysis was performed with β at 80% and α at 5% level. Goodness-of-fit statistics was used to evaluate the model fits.

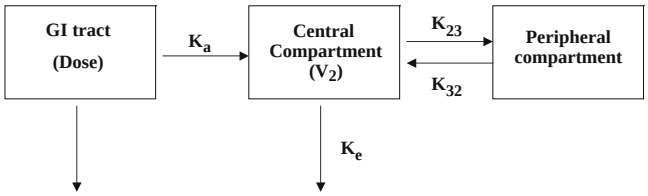

Fig. 1. A schematic of a two-compartment pharmacokinetic model for phenol red. Where K_a absorption rate constant, K_{23} and K_{32} distribution rate constants, V_2 volume of the central compartment, K_e elimination rate constant.

RESULTS

Absorption Enhancement of Phenol Red Upon Co-Administration with SDS

The IV and negative control oral absorption data was fitted to a two-compartment model depicted in Fig. 1, using WinNonlin software. Phenol red followed flip-flop kinetics i.e. the oral absorption rate constant (K_a) for phenol red was smaller than its elimination rate constant (K_e). The pharmacokinetic parameters determined for phenol red using both IV and oral study data are listed in Table I.

The oral absorption enhancement experiments were performed to ensure that the concentrations of SDS chosen (1% as treatment and 1.5 and 2% as positive controls), indeed caused significant increase in plasma concentrations for the marker molecules so that further experiments could be designed to measure absorption barrier recovery. SDS led to significantly higher plasma concentrations at all the three concentrations used (figure available online, see ESM). The observed C_{max}, T_{max} and AUC values for phenol red are listed in Table II. Higher C_{max} and AUC were achieved with increasing concentrations of SDS. An earlier T_{max} was obtained and it was seen to be about 10 min with all the three concentrations of SDS, showing that the penetration enhancement action of SDS was rapid. Since it was difficult to draw blood samples earlier than 10 min, an accurate T_{max} for the treatment groups could not be estimated. Mean residence time (MRT), mean absorption time (MAT) and bioavailability were determined by performing statistical moment analysis (Table II). MRT and MAT decreased with increasing dose of SDS indicating that the average time needed for absorption of phenol red decreased when co-administered with increasing amounts of SDS.

Pharmacokinetic evaluation of oral absorption of drugs with penetration enhancers is traditionally performed by statistical moment analysis. In the present study, it did show results that one would expect from a penetration enhancer and provided a way of comparison among the treatment groups. However, an interesting observation was made when the semi-log plots of mean plasma concentration-time profiles obtained for phenol red with SDS were overlaid with the IV plot (Fig. 2). The initial slope (from time 0 to about 60 min) for oral absorption curves of phenol red with SDS was similar to that of the IV curve, and after 60 min, the slopes were similar to that of the negative control plot. It was evident that initially the K_a values for SDS treated groups were higher than K_e and later became smaller than K_e. This trend could not be captured with non-compartment analysis and no reported literature was available that utilized pharmacokinetic modeling to show changes in K_a with time. To estimate changes in K_a, two-compartment analysis was performed on SDS treatment groups using MATLAB®5 software as described in "MATERIALS AND METHODS" with a step-function analysis. With microscopy, as described in the following section, it was noted that damage was caused to the duodenum instantaneously and maximally. In the jejunum damage occurred later and to a lesser extent. We assumed that as the oral gavage solution traveled down the intestinal tract, it experienced a different K_a depending upon the damage caused to the mucosal wall, with maximum K_a initially. The model fits obtained are shown in Fig. 3. The R^2 values obtained from the goodness-of-fit statistics ranged from 0.993 to 0.998. The absorption rate constant values (K_a) used to fit the two-compartment model, are depicted in Fig. 4 and are available online in a table format (see ESM). The results are summarized in Table III.

The two-compartment analysis showed that with all the concentrations of SDS, the absorption barrier was affected most in the first one hour (in the proximal region of the small intestine) giving large K_a values initially. The effect of SDS on the absorption barrier became lesser in subsequent hours (in the lower parts of the small intestine), resulting in smaller K_a values. With 1% SDS, K_a returned to the control value in 1 h. With 1.5 and 2% SDS, it required 2 and 4 h respectively. A comparison of the predicted K_a values obtained using a continuous function and a step function are depicted in Fig. 5A–C and values are summarized in Table III. As seen in the graphs, the K_a values predicted by a continuous function were within those determined by a step function analysis. More specifically, they were within 20% of those estimated from a step function analysis near the recovery times (1 h for 1% SDS, 2 h for 1.5% SDS and 4 h for 2% SDS). Goodness-of-fit statistics performed on the model fits showed that the R^2 values obtained ranged from 0.980 to 0.998.

Explaining the changes in K_a mathematically is a difficult challenge due to the complexity of the *in vivo* system coupled with the sparseness of the existing experimental data set (only seven data points per animal were obtained). Nonetheless the experimental data obtained could be adequately fit through the use of a two parameter exponentially time dependent K_a function and validated the K_a values estimated by model fitting with a step function.

Table I. Pharmacokinetic Parameters Estimated for Phenol Red

Pharmacokinetic parameters	Estimated values
K_e (min^1)	0.024±0.003
K_{23} (min^1)	0.0138±0.014
K_{32} (min^1)	0.01±0.004
V_2 (ml)	24 ml
K_a (first order oral absorption rate constant; min^1)	0.009±0.001
F (oral bioavailability; %)	1.5%±0.10

$n=4$ for IV bolus study and $n=12$ for oral absorption study. Each value represents mean ± SE.
K_e Elimination rate constant, K_{23} and K_{32} distribution rate constants, K_a first order absorption rate constant in the gastrointestinal tract and F percent oral bioavailability by fitting IV and oral absorption data to a two-compartment model

Table II. Effect of SDS on Oral Absorption of Phenol Red

Treatment group	C_{max} (mcg/ml)	T_{max} (min)	AUC ($t_{0300\ min}$)	MRT (min)	MAT (min)
Control	0.58±0.08	60±0	108.74±15.72	208.88±8.06	133.07±8.06
1% SDS	2.73±0.33*	13±2	294.22±30.44*	136.04±5.2*	60.23±5.2*
1.5% SDS	4.69±0.29*	UD	435.55±23.27*	99.80±3.06*	23.99±3.06*
2% SDS	7.86±0.75*	UD	665.25±26.03*	91.30±2.78*	15.49±2.78*

C_{max} Peak plasma concentration and T_{max} time for peak plasma concentration are the averages calculated from the observed data. AUC($t_{0-300\ min}$) area under the plasma concentration–time curve was calculated using the linear trapezoidal rule between time zero and 300 min. MRT mean residence time was calculated by extrapolating the AUC to infinity. MAT mean absorption time is the difference between MRT of the respective treatment group and that after intravenous administration. Control, n=12; SDS treatment, n=6. Values are expressed as mean ± SE.
UD Unable to determine
*$p<0.05$, statistically significant difference from the control values

Once absorption enhancement profiles were obtained for phenol red with SDS, recovery studies were performed after oral administration of SDS at 1, 1.5 and 2% concentrations.

Absorption Barrier Recovery

Results obtained for this set of experiments are summarized in Table IV (plasma concentration–time profiles available online, see ESM). Since actual experimental values were obtained until 300 min, AUC values were calculated only until 300 minutes and were not extrapolated to infinity. C_{max}, AUC, MRT and MAT values decreased and T_{max} increased with increasing length of recovery times. After 15 and 30-min recovery periods, the pharmacokinetic parameters for phenol red were still significantly different from the negative control indicating that absorption barrier recovery was partial. After 1-h recovery period, the pharmacokinetic parameters were statistically comparable to those of the negative control. This observation was confirmed by performing 3-h recovery experiments. The results indicated that absorption barrier recovery as measured against phenol red was complete for 1% SDS in 1 h.

The C_{max}, T_{max}, AUC, MRT and MAT for 1 h recovery groups for 1% SDS were statistically comparable at 0.05 significance level, when six animals were used per group. This indicated that absorption barrier properties measured against phenol red were similar after recovery as compared to those of the negative control. To make sure that the difference in data for these groups is solely due to individual variability and not due to difference in the treatment, power analysis was performed at 80% and significance level of 5%. The number of animals required for each experimental group was calculated to be 12. Hence, 12 rats were used each for 1-h recovery group with 1% SDS and the negative control group.

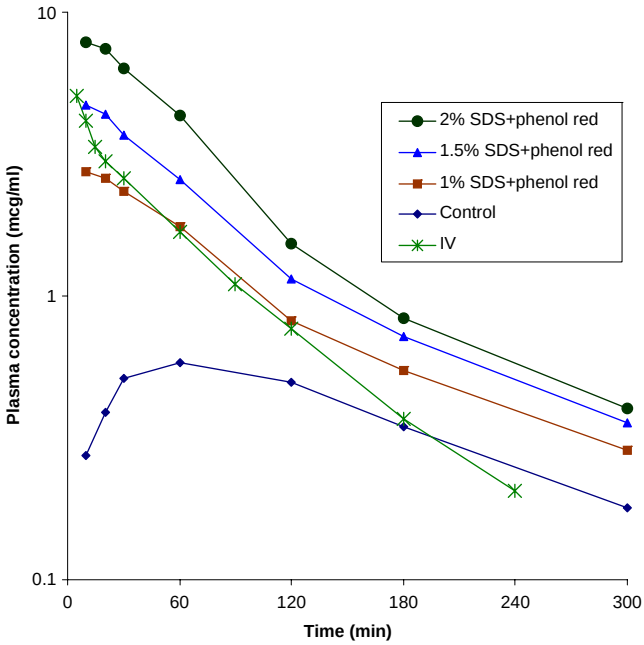

Fig. 2. Overlay of semi-logarithmic plots of plasma concentrations of phenol red after IV bolus administration and oral administration with and without SDS.

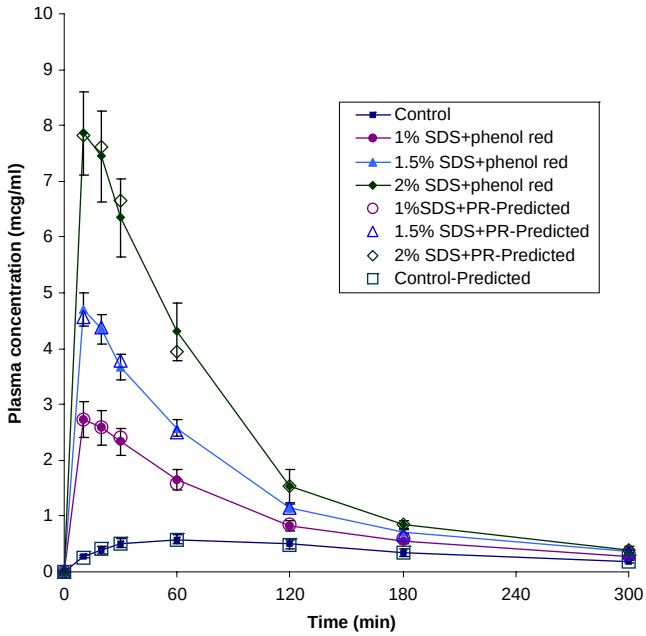

Fig. 3. Observed and predicted plasma concentrations obtained by two-compartment model fitting using a step–function analysis for phenol red when orally administered with and without SDS.

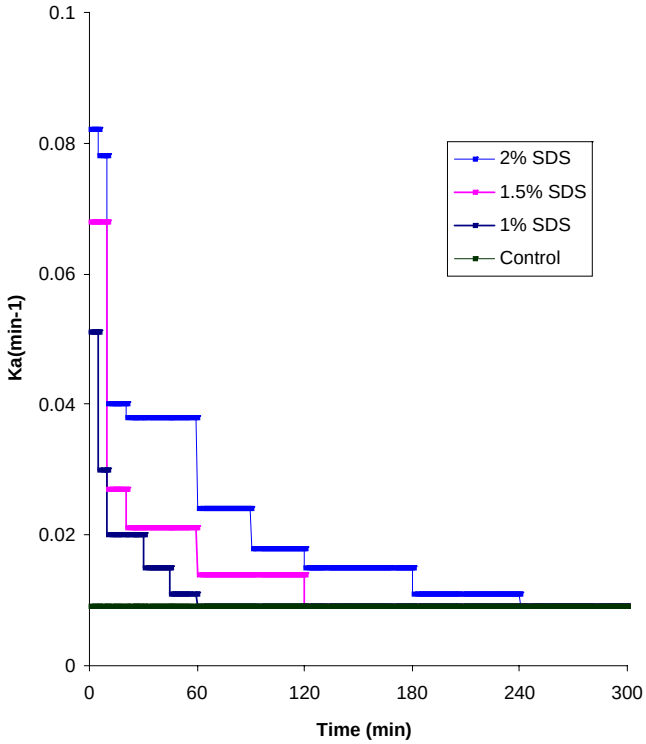

Fig. 4. Change in oral absorption rate constant (K_a) of phenol red with respect to time when co-administered with SDS, as estimated by two-compartment model fitting using a step-function analysis.

Three-hour recovery experiments were performed for the positive control SDS concentrations. Results are summarized in Table IV (figures available online, see ESM). C_{max}, T_{max}, AUC, MRT and MAT for 1 and 1.5% SDS treated groups after 3-h recovery are statistically comparable to the negative control, whereas for 2% SDS, C_{max} and AUC were significantly higher, T_{max} was earlier and MRT and MAT were shorter, suggesting that recovery was not complete by 3 h for 2% SDS.

Model fits obtained from two-compartment analysis on recovery data using MATLAB®5 are shown in Fig. 6A, B. The changes in K_a with respect to time are shown in Fig. 7A, B. The absorption rate constant (K_a) for phenol red when administered 15 min after 1% SDS, returned to the control value after 45 min (1 h after administration of 1% SDS) whereas K_a for phenol red when administered 30 min after 1% SDS, returned to the control value after 30 min (similar total recovery time of 1 h after administration of 1% SDS). For the 1-h recovery group, K_a was comparable to that of the control group. In 3-h recovery groups, with 1 and 1.5% SDS treatments, K_a was comparable to the control value whereas with 2% SDS treatment, it took an additional 1 h for K_a to return to the control value (a total 4 h recovery time was required). See Table III.

As described in the previous section, the two-compartment pharmacokinetic analysis on phenol red data obtained after co-administration with SDS, revealed that for 1 and 1.5% SDS, the K_a came back to the control value in one hour and 2 h respectively, whereas it took 4 h for 2% SDS. The experiments designed for absorption barrier recovery were in agreement with these results. K_a estimated using a step function analysis for 15 and 30 min recovery experiments with 1% SDS and 3 h recovery experiment with 2% SDS were in accordance with the K_a's estimated at the corresponding time points using both step and continuous functions described for absorption enhancement experiments.

Recovery of Morphology

Morphological recovery was observed using light and transmission electron microscopy in the duodenum and jejunum. Figure 8A presents a cross section of control duodenal villi. Normal intestinal epithelium is observed with well-aligned viable epithelial cells. The action of SDS on the duodenum was rapid. The duodenal villi showed signs of injury at both 10 and 15 min after administration of 1% SDS (results for 15 min are given in Fig. 8B). The villi were swollen and ruptured with damage extending to the lamina propria. Thirty minutes after administration of 1% SDS, the damaged area on the villi looked partially covered by the epithelial cells (Fig. 8C). One hour after administration of 1% SDS the duodenal villi were covered with a continuous layer of epithelial cells. Light microscopy (LM) results showed complete morphological recovery after 1 h of treatment with 1% SDS for the duodenum (Fig. 8D). Results for jejunum observed with light microscopy are shown in Fig. 8E–G. Figure 8E shows normal jejunal villi covered with a contin-

Table III. Comparison of Changes in Absorption Rate Constant of Phenol Red Upon SDS Administration as Estimated Using a Step–function Analysis

Treatment group	K_a (maximum; min^1)	Time of recovery estimated by curve fitting
Control	0.009	–
1% SDS	0.051	1 h
1.5% SDS	0.068	2 h
2% SDS	0.082	4 h
1% SDS–15 min recovery	0.027	45 min (+15 min recovery) = 1 h
1% SDS–30 min recovery	0.020	30 min (+30 min recovery) = 1 h
1% SDS–1 h recovery	0.009	1 h
1.5% SDS–3 h recovery	0.009	<3 h
2% SDS–3 h recovery	0.014	1 h (+3 h recovery=4 h)

K_a (maximum) is the maximum value of the K_a first order absorption rate constant, estimated for each treatment by curve fitting using step-function analysis.

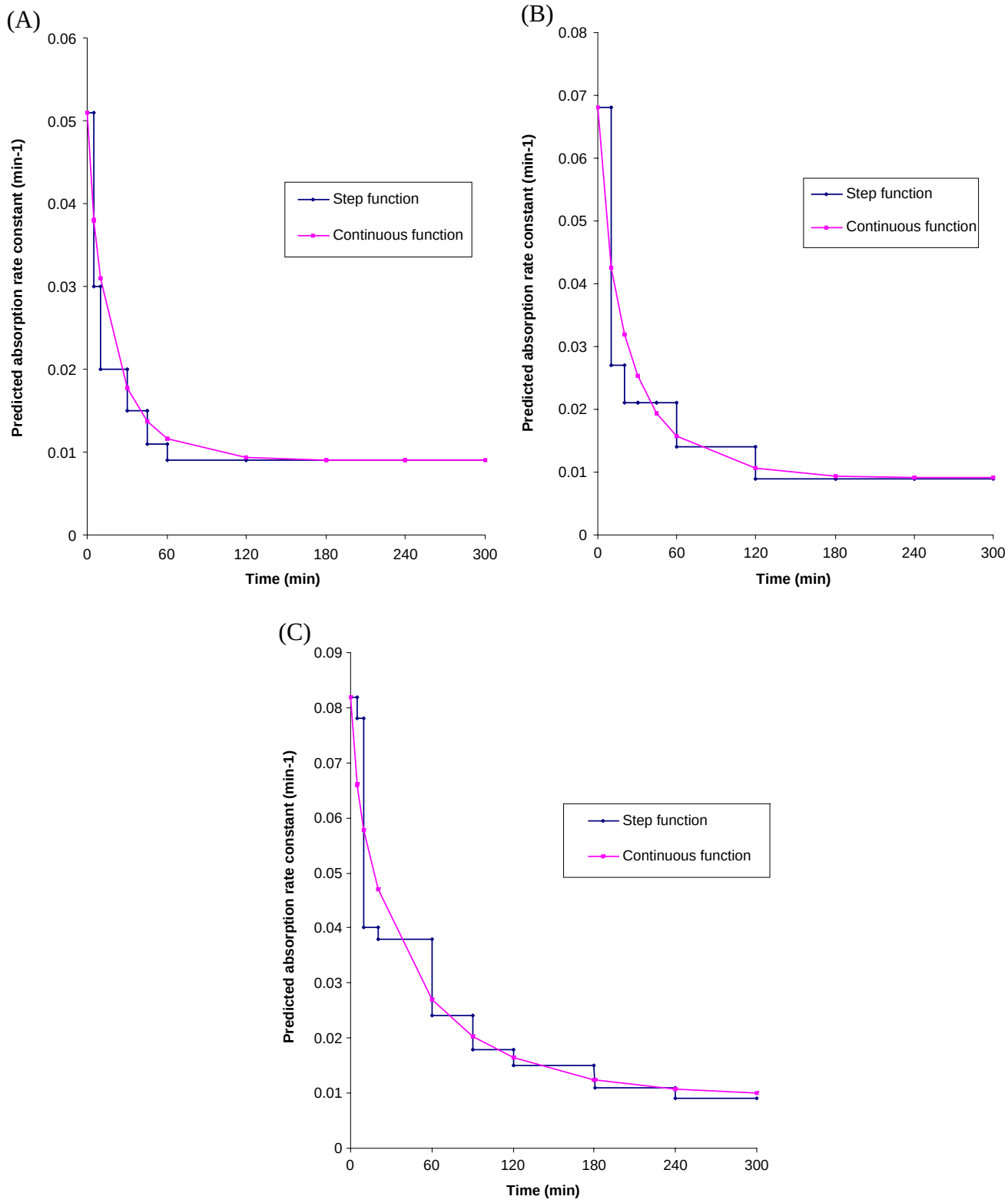

Fig. 5. Estimation of K_a using a continuous exponential function. **A** The following equation with two variables a and b were used to model K_a for 1% SDS treatment. $K_a = Ka_0 + A*\exp(-a*\text{time}^b)$, Where K_a = predicted absorption rate constant, K_{a0} = control K_a (0.009 min^{-1}), A = 0.042 (taken from step function analysis and held constant to reduce the number of variables). $a = 0.1$, $b = 0.81$. **B** The following equation with two variables a and b were used to model K_a for 1.5% SDS treatment. $K_a = Ka_0 + A*\exp(-a*\text{time}^b)$, Where K_a = predicted absorption rate constant, K_{a0} = control K_a (0.009 min^{-1}), $A = 0.059$ (taken from step function analysis and held constant to reduce the number of variables), a = 0.1, $b = 0.75$. **C** The following equation with two variables a and b were used to model K_a for 2% SDS treatment. $K_a = Ka_0 + A*\exp(-a*\text{time}^b)$, where K_a = predicted absorption rate constant, K_{a0} = control K_a (0.009 min^{-1}), $A = 0.073$ (taken from step function analysis and held constant to reduce the number of variables), $a = 0.08$, $b = 0.7$.

Table IV. Oral Absorption of Phenol Red After Different Recovery Periods Upon Administration of SDS

Treatment group	C_{max} (mcg/ml)	T_{max} (min)	AUC ($t_{0300\ min}$)	MRT (min)	MAT (min)
1% SDS	2.73±0.33*	13±2	294.22±30.44*	136.04±5.2*	60.23±5.2*
1% SDS–15 min recovery	1.78±0.17*	24±2	241.60±20.81*	152.07±4.7 *	76.27±4.7*
1% SDS–30 min recovery	1.10±0.10*	31±6	167.61±13.13*	159.86±3.31*	84.05±3.31*
1% SDS–1 h recovery	0.60±0.06	60±0	110.85±11.65	208.83±9.4	133.02±9.4
1% SDS–3 h recovery	0.68±0.08	60±0	130.58±15.56	200.43±8.76	124.62±8.76
1.5% SDS–3 h recovery	0.76±0.08	60±0	148.28±14.86	203.01±22.49	127.20±22.49
2% SDS–3 h recovery	1.11±0.07*	40±7	228.63±15.46*	159.76±13.25*	83.95±13.25*
Control	0.58±0.08	60±0	108.74±15.72	208.88±8.06	133.07±8.06

C_{max} peak plasma concentration and T_{max} time for peak plasma concentration are the averages calculated from the observed data. AUC($t_{0–300\ min}$) area under the plasma concentration-time curve was calculated using the linear trapezoidal rule between time zero and 300 min. MRT mean residence time was calculated by extrapolating the AUC to infinity. MAT mean absorption time is the difference between MRT of the respective treatment group and that after intravenous administration. Control and 1% SDS–1 h recovery, $n=12$; other treatments, $n=6$. Values are expressed as mean ± SE.
*$p<0.05$, statistically significant difference from the control values.

uous monolayer of epithelium. Damage was evident in the jejunum only after 15 min (Fig. 8F). The intercellular spaces were dilated. Note that damage is not as extensive in the jejunum as it is seen in the duodenum at the same time. The morphology looked normal for the jejunal villi 30 min after administration of 1% SDS under a light microscope (Fig. 8G).

The morphological recovery results were further confirmed with transmission electron microscopy (TEM; Fig. 9A–I). The control duodenal epithelium showed a surface covered with tall microvilli and normal tight and adherens junctions between the normal duodenal epithelial cells (Fig. 9A, B). For duodenal tissues obtained 30 min after treatment with 1% SDS, the epithelia surrounding the area of damage were observed under TEM. They had fewer microvilli on the surface and there were no defined junctional complexes on the epithelial surface facing the damage (Fig. 9C, D). Figure 9E, F shows appearance of duodenal epithelium one hour after treatment with SDS. The microvilli have started to regenerate and the paracellular junctions have also started to reform. Even though the microvilli are not as tall as those seen for the control samples, the plasma membrane looks continuous and covered with microvilli. This implies that the zone of injury is covered with intact epithelia. Figure 9G, H shows normal jejunal epithelium covered with normal tall microvilli and normal tight and adherens junctions. Thirty minutes after treatment with 1% SDS, the paracellular junctions in the jejunum looked normal as shown in Fig. 9I.

DISCUSSION

Damage and recovery studies pertaining to penetration enhancers have been performed using *in vitro*, *in situ* and *in vivo* models. *In vitro* models are particularly attractive because the mechanisms of damage and recovery are easily probed and relatively cleaner samples are obtained for analysis (49–51). However, the recovery times are highly dependent upon the type of model used in the study. For example, when the rabbit jejunum was treated with 0.5 mM chenodeoxycholate for 25 min in an *in vitro* system, mucosal permeability to lactulose returned to the normal value after 40 min (52). Similarly, when the guinea pig ileum was exposed to 0.06% Triton-X 100 (0.75 mM) for 5 min in an *in vitro* model, it took one hour for the tissue to seal the defect, when observed under a light microscope (53). Whereas in an *in situ* perfusion model, when the small intestine of rat was perfused with 20 mM deoxycholate for 30 min, it took one hour to cover the denuded villus tips with epithelium, when observed under a light microscope (54). In a similar study by Argenzio *et al*. acute injury caused to porcine colon by a concentration of 15 mM deoxycholate for 30 min, was repaired by flattened migrating cells returning mannitol permeability to normal within 40 min (55). In all the studies listed above, even though the recovery time was 40–60 min, it should be noted that the concentration of surfactant used in the *in situ* perfusion studies was much higher compared to those used for the *in vitro* models. The repair in the *in situ* models was much quicker considering the high amount of chemicals used to inflict injury, owing probably to the live tissue and the intact blood supply. Recovery times are also dependent on contact time between the tissue or cells and the penetration enhancer. In a caco-2 cell model, 0.4 mM SDS exposure for 20 min resulted in reversible permeation enhancement of mannitol, 1-deamino-8-D-arginine-vasopressin and polyethylene glycol 4000. The cell model recovered within 2–3 h after the buffer containing 0.4 mM SDS was replaced with culture medium, whereas a longer exposure time of 2 h resulted in irreversible change in permeation (46).

To avoid these variables and to obtain realistic estimates of recovery times, an *in vivo* model was selected for this study. Since absorption enhancers act by altering the barrier properties of the membrane, measuring absorption kinetics of a marker through damaged and recovered gut would give a direct measure of functional recovery of the gastrointestinal mucosa. We selected phenol red, a highly polar, poorly absorbed and relatively small molecule, as a marker. We were able to show absorption barrier recovery quantitatively in terms of pharmacokinetic parameters of phenol red (C_{max}, T_{max}, AUC, MRT and MAT). Even though statistical moment analysis is routinely employed for pharmacokinetic analysis of oral enhancement data, we found that it is not adequate to provide useful insights into changes in the rate of absorption with respective to time. Phenol red is a poorly absorbed

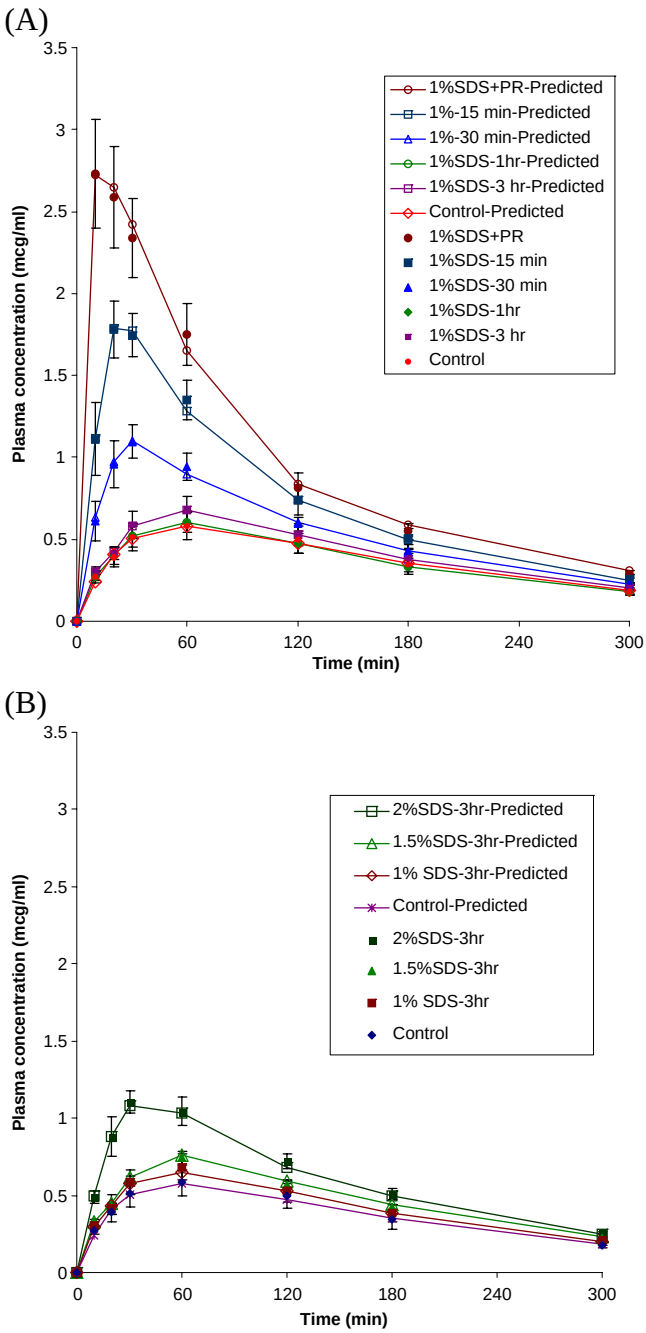

Fig. 6. Observed and predicted plasma concentrations obtained by two-compartment model fitting using a step–function analysis for oral absorption of phenol red **A** after different recovery times upon administration of 1% SDS **B** after 3-h recovery period upon administration of SDS.

marker with its absorption pathway mainly restricted to the paracellular spaces due its highly polar nature (40–43). Normally, its oral pharmacokinetics should exhibit flip-flop kinetics i.e. the terminal slope of semi-log plot of mean plasma concentration-time profile should reflect K_a rather than K_e. The semi-log plot (Fig. 2) showed that the oral absorption curves for the SDS treated groups reflected the elimination phase and tended to parallel the terminal IV curve for the initial 1–2 h, implying that the K_a values for SDS treated groups were higher than K_e during this time. At later time points, K_a became smaller than K_e such that the curves tended to parallel the negative control oral absorption plot, showing flip-flop kinetics. To elucidate this trend, we estimated changes in K_a with respect to time by fitting the

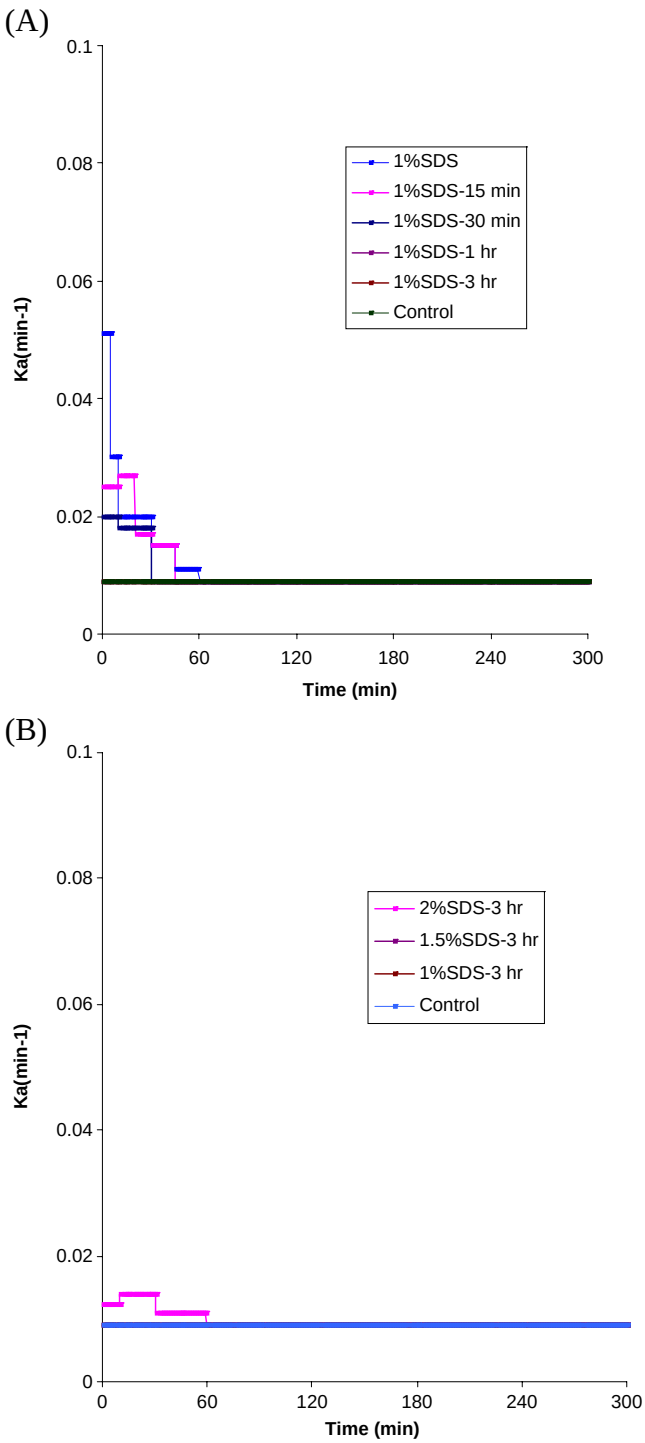

Fig. 7. Change in oral absorption rate constant (K_a) with respect to time as estimated by two-compartment model fitting using a step–function analysis for phenol red **A** after different recovery times upon administration of 1% SDS **B** after a 3-h recovery upon administration of SDS (plots of K_a *vs* time for control, 1% SDS–3 h and 1.5% SDS–3 h recovery overlap).

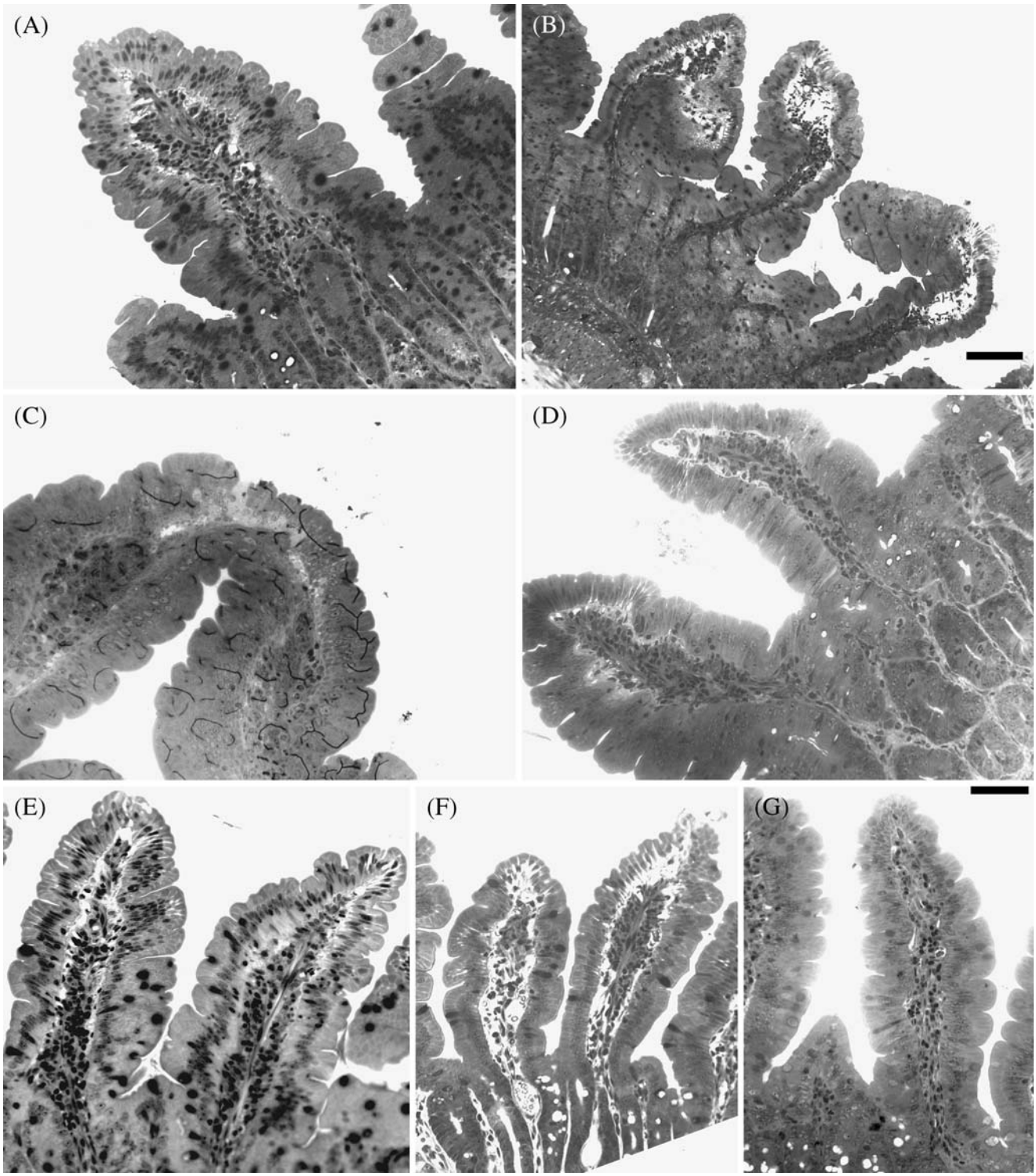

Fig. 8. Light microscopy (scalebar = 100 μm). **A** Control duodenum–normal intestinal epithelium is observed, with well-aligned viable epithelial cells covering the surface of the villi. **B** Duodenum 15 min after administration of 1% SDS–villi are swollen and ruptured with damage extending to the lamina propria. The damaged epithelial cells are being sloughed off from the villus surface. **C** Duodenum 30 min after administration of 1% SDS–villi are partially covered by the epithelial cells as compared to the villi 10 and 15 min after the treatment. **D** Duodenum 1 h after administration of 1% SDS–villi are covered with a continuous layer of epithelial cells appear normal. **E** Control jejunum–villi are normal with a continuous layer of epithelial cells on the surface. **F** Jejunum 15 min after administration of 1% SDS—the intercellular spaces in the epithelium are dilated especially at the tip of the villi. The effect of SDS on the jejunum is not as drastic as seen in the duodenum. **G** Jejunum 30 min after administration of 1% SDS–villi look normal with a continuous layer of epithelium on the surface.

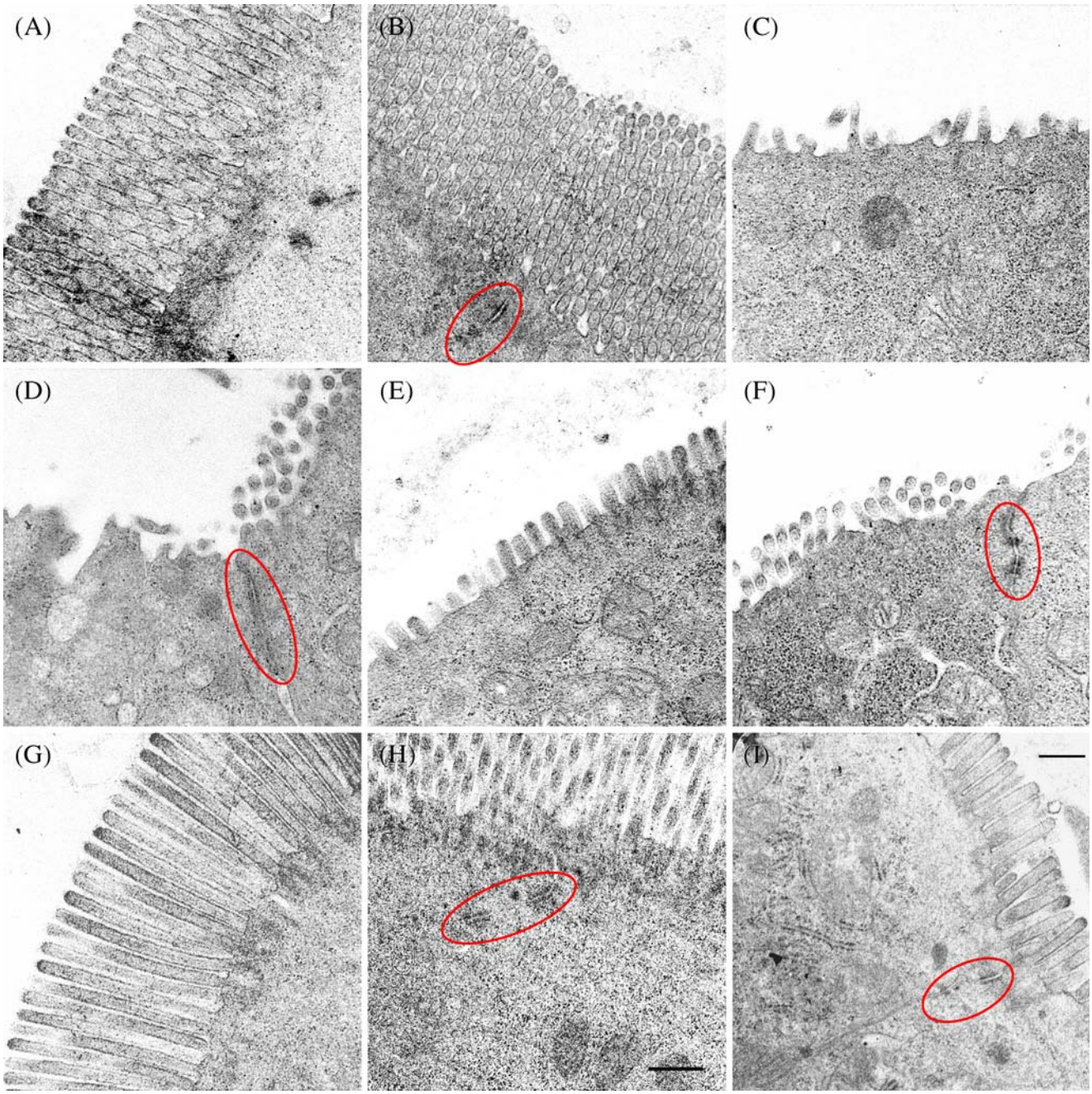

Fig. 9. Transmission electron microscopy (scalebar = 500 nm). The areas of junctional complexes are *circled red* in the figures. **A** and **B** Control duodenum—the epithelial cell surface is covered with tall microvilli and the junctional complexes appear normal. **C** and **D** Duodenum 30 min after treatment with 1% SDS—there is a substantial loss of microvilli from the surfaces of epithelial cells at or bordering the zones of injury. Remaining microvilli are shortened and many appear damaged. Junctional complexes between neighboring epithelial cells in the area are abnormal or absent, consistent with the restitution process. **E** and **F** Duodenum 60 min after treatment with 1% SDS—the epithelial cells at the tip of the villi have started to regenerate microvilli on the luminal surface and the junctional complexes with the adjacent epithelial cell are reorganizing. **G** and **H** Control jejunum—the luminal surface of the epithelium is covered with tall microvilli and the junctional complexes look normal. **I** Jejunum 30 min after treatment with 1% SDS—the luminal surface of epithelial cells at the tip of the villi is covered with microvilli and the junctional complexes are well formed.

phenol red data to a two-compartment model using MATLAB®5 software. Two-compartment modeling proved to be a useful tool since it allowed the measurement of functional recovery (absorption barrier recovery) temporally. The model fits revealed that at all the three concentrations, the action of SDS on the intestinal mucosa was almost instantaneous, giving rise to the highest K_a values in the beginning. The K_a reduced with time, as the mucosa recovered and it came to the control level in 1, 2 and 4 h for 1, 1.5 and 2% SDS respectively.

Two important findings of this study were: K_a changed with time after damage inflicted by the penetration enhancer and recovery time determination in terms of K_a was possible from a single set of experiments (absorption enhancement

experiments). Estimating K_a *versus* time also offers a point-to-point input of changes in mucosal permeability during damage and subsequent recovery. Experiments designed for absorption barrier recovery studies corroborated these results, showing that measuring absorption rate constant of a marker was a valid and robust method to determine recovery of the barrier function of the gastrointestinal mucosa.

The findings from the absorption barrier recovery study were supplemented with a more traditional method, morphological evaluation. The crucial step following disruption of the gastrointestinal epithelium is covering of the denuded area by epithelial cells to rapidly re-establish the intrinsic barrier. This is accomplished by a process called restitution, in which, the viable epithelial cells surrounding the area of defect flatten and begin to spread by extending pseudopod-like structures called lammelipodia. The cells lose apical-basolateral polarity by undergoing brush border and junctional disassembly. The cells become polarized along the leading edge, forming a contractile purse-string of actomyosin cables. This actin–myosin purse-string draws the flattened epithelial cells forward over the exposed area. Matovelo *et al*. (56) demonstrated this process using immunofluorescent staining of cytokeratin and actin. Once cell-to-cell contact is established, junctional complexes are reformed and the microvilli start to re-grow. This is a rapid, first-aid mechanism to cover defects in the barrier and does not involve epithelial cell proliferation (57–58). Intestinal tissue damage due to surface-active agents and subsequent recovery due to restitution process have been reported in several studies. Waller *et al.* (59) observed that repair via epithelial restitution occurred in the large intestine of the rat, in 2 h following insult with 25 mM sodium deoxycholate. Similar observations were made by Millan *et al*. (29) in normal humans using histology, where damage in the small intestine caused by ethanol recovered in 2 h. Recovery due to restitution in rat rectal epithelium after treatment with deoxycholate and SDS has been described by Nakanishi et al. (60). Rapid barrier restitution was noted by Moore, Carlson and Madara in the small intestine of guinea pig after exposure to Triton X-100. The authors showed that both villus contraction and epithelial cell migration were responsible for closing the denuded area (53,61).

In the present investigation, the changes seen in morphology after SDS administration were consistent with the reported studies (Figs. 8 and 9). Damage was evident in the duodenum 10 to 15 min after treatment with 1% SDS due to its solubilizing action on the epithelial membrane components like phospholipids and proteins (44,45). The damaged cells probably died of necrosis and were sloughed off from the villi into the lumen. As a result, discontinuity in the duodenal epithelial layer was observed. Thirty minutes after treatment with 1% SDS, partial recovery was seen in the duodenum in light microscopy and the epithelial cells bordering the zone of injury did not show junctional complexes and microvilli in TEM images, indicating that these cells were involved in restitution process. Light microscopy images revealed that repair was complete in 1 h in the duodenum. The villi looked normal and were completely covered with epithelium. The TEM images showed that the junctional complexes had started to re-establish and the luminal surface of the epithelium had started to show growth of microvilli.

SDS acts on the transcellular route above the critical micellar concentration (CMC, 6–8 mM) by extracting membrane components namely proteins and lipids (62–63). Below the CMC, SDS acts mainly on the paracellular junctions and disrupts them (46). This was demonstrated convincingly by Hurni *et al*. with Sodium taurodihydrofusidate (STDHF). Using confocal laser scanning microscopy, Hurni *et al*. (64) showed that at 1.6 mM concentration (below its CMC of 2.5 mM), STDHF increased permeability of fluorescently labeled Dextran 4000 (FD4) paracellularly whereas at 8 mM concentration it increased permeability of FD4 both para- and transcellulary. In the present study, the membrane solubilizing action of SDS on the epithelium was confined to the duodenum whereas only the paracellular spaces were affected in the jejunum (Fig. 8F). Although the SDS concentration was not measured in this study, based on the reported literature (46,62–64) and our observations, we speculate that the membrane solubilizing action of SDS was seen in the duodenum due to the large concentration of SDS administered as an oral gavage. As the gavage solution traveled down to the jejunum, the concentration of SDS was reduced (below the CMC) so that the action was limited to the paracellular pathway. Hudspeth *et al*. (65) showed that when injured, paracellular spaces could be repaired within 30 min *in vitro*. In this study we found that it took 15–30 min to repair the paracellular junctions in rat jejunum *in vivo*.

Numerous studies have demonstrated that the absorption barrier recovery takes place in conjunction with morphological recovery (66–68). In this study, morphological recovery showed a good correlation with functional recovery. Maximum damage seen in microscopy coincided with a tenfold increase in plasma concentration of phenol red and the highest K_a in the first 10 min. As morphological recovery advanced, K_a became progressively smaller. When K_a reached the baseline value (at 60 min), morphology looked normal.

To conclude, despite decades of work performed on penetration enhancers, they have not found practical utility in formulations due to safety concerns. These concerns originated from lack of understanding in how penetration enhancers affect the barrier function of the gastrointestinal mucosa partly because of inability to quantify the effect. This work was attempted to fill this gap in understanding by establishing a pharmacokinetic method to evaluate functional recovery of the gastrointestinal mucosa dynamically, after use of a penetration enhancer. We found that it is possible to achieve absorption enhancement with temporary and reversible alteration of mucosal barrier properties. The changes noted in absorption of marker molecules as a result of treatment with a penetration enhancer and the subsequent recovery were in accordance with morphological changes observed using microscopy techniques. These results will hopefully help in better design of future studies involving use of penetration enhancers and in a better understanding of their effects on the mucosal membrane.

REFERENCES

1. D. C. Baumgart and A. U. Dignass. Intestinal barrier function. *Curr. Opin. Clin. Nutr. Metab. Care* **5**:685–694 (2002).
2. G. L. Eastwood. Gastrointestinal epithelial renewal. *Gastroenterology* **72**:962–975 (1977).

3. M. Lipkin. Proliferation and differentiation of gastrointestinal cells. *Physiol. Rev* **53**:891–915 (1973).
4. D. W. Powell. Barrier function of epithelia. *Am. J. Physiol* **241**: G275–G288 (1981).
5. A. L. Daugherty and R. J. Mrsny. Regulation of the intestinal epithelial paracellular barrier. *Pharm. Sci. Technol. Today* **2**:281–287 (1999).
6. K. L. Lutz and T. J. Siahaan. Molecular structure of the apical junction complex and its contribution to the paracellular barrier. *J. Pharm. Sci* **86**:977–984 (1997).
7. J. P. Kraehenbuhl, E. Pringault, and M. R. Neutra. Intestinal epithelia and barrier functions. *Aliment. Pharmacol. Ther* **11**:3–8 (1997).
8. T. Z. Csaky. Intestinal permeation and permeability: an Overview. In T. Z. Csaky (ed.), *Pharmacology of Intestinal Permeation*, Springer, New York, 1984, pp. 51–59.
9. A. Allen, G. Flemstrom, A. Garner, and E. Kivilaakso. Gastroduodenal mucosal protection. *Physiol. Rev* **73**:823–857 (1993).
10. E. Engel, P. H. Guth, Y. Nishizaki, and J. D. Kaunitz. Barrier function of the gastric mucus gel. *Am. J. Physiol* **269**:G994–G999 (1995).
11. M. Goke, and D. K. Podolsky. Regulation of the mucosal epithelial barrier. *Baillieres Clin. Gastroenterol* **10**:393–405 (1996).
12. J. S. Trier. The surface coat of the gastrointestinal epithelial cells. *Gastroenterology* **56**:618–624 (1969).
13. J. Meyer-Kirchrath and K. Schror. Cyclooxygenase-2 inhibition and side-effects of non-steroidal anti-inflammatory drugs in the gastrointestinal tract. *Curr. Med. Chem* **7**:1121–1129 (2000).
14. R. I. Russell. Protective effects of the prostaglandins on the gastric mucosa. *Am. J. Med* **81**:2–4 (1986).
15. R. Rao and F. Porreca. Epidermal growth factor protects mouse ileal mucosa from Triton X-100-induced injury. *Eur. J. Pharmacol* **303**:209–212 (1996).
16. B. Montaner, M. Asbert, and R. Perez-Tomas. Immunolocalization of transforming growth factor-alpha and epidermal growth factor receptor in the rat gastroduodenal area. *Dig. Dis. Sci* **44**:1408–1416 (1999).
17. H. Steiling and S. Werner. Fibroblast growth factors: key players in epithelial morphogenesis, repair and cytoprotection. *Curr. Opin. Biotechnol* **14**:533–537 (2003).
18. Y. Choda, Y. Morimoto, H. Miyaso, S. Shinoura, S. Saito, T. Yagi, H. Iwagaki, and N. Tanaka. Failure of the gut barrier system enhances liver injury in rats: protection of hepatocytes by gut-derived hepatocyte growth factor. *Eur. J. Gastroenterol. Hepatol* **16**:1017–1025 (2004).
19. L. Thim. Trefoil peptides: from structure to function. *Cell Mol. Life Sci* **53**:888–903 (1997).
20. A. Andoh, K. Kinoshita, I. Rosenberg, and D. K. Podolsky. Intestinal trefoil factor induces decay-accelerating factor expression and enhances the protective activities against complement activation in intestinal epithelial cells. *J. Immunol* **167**:3887–3893 (2001).
21. S. Fagarasan and T. Honjo. Regulation of IgA synthesis at mucosal surfaces. *Curr. Opin. Immunol* **16**:277–283 (2004).
22. S. J. Golby and J. Spencer. Where do IgA plasma cells in the gut come from?. *Gut* **51**:150–151 (2002).
23. B. M. Myers, J. L. Smith, and D. Y. Graham. Effect of red pepper and black pepper on the stomach. *Am. J. Gastroenterol* **82**(3):211–214 (1987).
24. E. Jensen-Jarolim, L. Gajdzik, I. Haberl, D. Kraft, O. Scheiner, and J. Graf. Hot spices influence permeability of human intestinal epithelial monolayers. *J. Nutr* **128**:577–581 (1998).
25. T. Hoshino, N. Kashimoto, and S. Kasuga. Effects of garlic preparations on the gastrointestinal mucosa. *J. Nutr* **131**no. Suppl 3, 1109S–1113S (2001).
26. H. Amagase, B. L. Petesch, H. Matsuura, S. Kasuga, and Y. Itakura. Intake of garlic and its bioactive components. *J. Nutr* **131**(Suppl 3):955S–962S (2001).
27. P. R. Kvietys, R. D. Specian, M. B. Grisham, and P. Tso. Jejunal mucosal injury and restitution: role of hydrolytic products of food digestion. *Am. J. Physiol* **261**:G384–G391 (1991).
28. R. P. Bird and W. R. Bruce. Effect of dietary calcium on the toxicity of bile acid and orally administered fat to colonic epithelium. *Prog. Clin. Biol. Res* **222**:487–494 (1986).
29. M. S. Millan, G. P. Morris, I. T. Beck, and J. T. Henson. Villous damage induced by suction biopsy and by acute ethanol intake in normal human small intestine. *Dig. Dis. Sci* **25**:513–525 (1980).
30. E. R. Lacy, G. P. Morris, and M. M. Cohen. Rapid repair of the surface epithelium in human gastric mucosa after acute superficial injury. *J. Clin. Gastroenterol* **17**(Suppl 1):S125–S135 (1993).
31. C. Aalykke and K. Lauritsen. Epidemiology of NSAID-related gastroduodenal mucosal injury. *Best Pract. Res. Clin. Gastroenterol* **15**:705–722 (2001).
32. J. L. Wallace. Pathogenesis of NSAID-induced gastroduodenal mucosal injury. *Best Pract. Res. Clin. Gastroenterol* **15**:691–703 (2001).
33. J. F. Bretagne, N. Vidon, C. L'Hirondel, and J. J. Bernier. Increased cell loss in the human jejunum induced by laxatives (ricinoleic acid, dioctyl sodium sulphosuccinate, magnesium sulphate, bile salts). *Gut* **22**:264–269 (1981).
34. K. J. Moriarty, M. J. Kelly, R. Beetham, and M. L. Clark. Studies on the mechanism of action of dioctyl sodium sulphosuccinate in the human jejunum. *Gut* **26**:1008–1013 (1985).
35. D. R. Saunders, J. Sillery, and D. Rachmilewitz. Effect of dioctyl sodium sulfosuccinate on structure and function of rodent and human intestine. *Gastroenterology* **69**:380–386 (1975).
36. T. Murakami, Y. Sasaki, R. Yamajo, and N. Yata. Effect of bile salts on the rectal absorption of sodium ampicillin in rats. *Chem. Pharm. Bull. (Tokyo)* **32**(5):1948–1955 (1984).
37. A. Fasano, G. Budillon, S. Guandalini, R. Cuomo, G. Parrilli, A. M. Cangiotti, M. Morroni, and A. Rubino. Bile acids reversible effects on small intestinal permeability—an *in vitro* study in the rabbit. *Dig. Dis. Sci* **35**:801–808 (1990).
38. V. S. Chadwick, T. S. Gaginella, G. L. Carlson, J. C. Debongnie, S. F. Phillips, and A. F. Hofmann. Effect of molecular structure on bile acid-induced alterations in absorptive function, permeability, and morphology in the perfused rabbit colon. *J. Lab. Clin. Med* **94**:661–674 (1979).
39. J. E. F. Reynolds (ed.). In Martindale, the extra pharmacopoeiaThe Royal Pharmaceutical Society of Great Britain, London, 1989, pp. 1555–1556.
40. K. Hosoya, H. Kubo, H. Natsume, K. Sugibayashi, and Y. Morimoto. Evaluation of enhancers to increase nasal absorption using Ussing chamber technique. *Biol. Pharm. Bull* **17**:316–322 (1994).
41. E. S. Swenson, W. B. Milisen, and W. Curatolo. Intestinal permeability enhancement: efficacy, acute local toxicity, and reversibility. *Pharm. Res* **11**:1132–1142 (1994).
42. M. Nakamaru, Y. Masubuchi, S. Narimatsu, S. Awazu, and T. Horie. Evaluation of damaged small intestine of mouse following methotrexate administration. *Cancer Chemother.Pharmacol* **41**:98–102 (1998).
43. A. Yamamoto, T. Uchiyama, R. Nishikawa, T. Fujita, and S. Muranishi. Effectiveness and toxicity screening of various absorption enhancers in the rat small intestine: effects of absorption enhancers on the intestinal absorption of phenol red and the release of protein and phospholipids from the intestinal membrane. *J. Pharm. Pharmacol* **48**:1285–1289 (1996).
44. K. Higaki, T. Yata, M. Sone, K. Ogawara, and T. Kimura. Estimation of absorption enhancement by medium-chain fatty acids in rat large intestine. *Res. Commun. Mol. Pathol. Pharmacol* **109**:231–240 (2001).
45. M. Sakai, T. Imai, H. Ohtake, and M. Otagiri. Cytotoxicity of absorption enhancers in Caco-2 cell monolayers. *J. Pharm. Pharmacol* **50**:1101–1108 (1998).
46. E. K. Anderberg and P. Artursson. Epithelial transport of drugs in cell culture. VIII: effects of sodium dodecyl sulfate on cell membrane and tight junction permeability in human intestinal epithelial (Caco-2) cells. *J. Pharm. Sci* **82**:392–398 (1993).
47. A. I. Walker, V. K. Brown, L. W. Ferrigan, R. G. Pickering, and D. A. Williams. Toxicity of sodium lauryl sulphate, sodium lauryl ethoxysulphate and corresponding surfactants derived from synthetic alcohols. *Food Cosmet. Toxicol* **5**:763–769 (1967).
48. O. G. Fitzhugh and A. A. Nelson. Chronic oral toxicities of surface-active agents. *J. Am. Pharmacol. Assoc* **37**:29–32 (1948).
49. H. Bohets, P. Annaert, G. Mannens, L. Van Beijsterveldt, K. Anciaux, P. Verboven, W. Meuldermans, and K. Lavrijsen.

Strategies for absorption screening in drug discovery and development. *Curr. Top. Med. Chem* **1**:367–383 (2001).
50. Y. Sambuy, I. De Angelis, G. Ranaldi, M. L. Scarino, A. Stammati, and F. Zucco. The Caco-2 cell line as a model of the intestinal barrier: influence of cell and culture-related factors on Caco-2 cell functional characteristics. *Cell Biol.Toxicol* **21**:1–26 (2005).
51. P. Artursson, K. Palm, and K. Luthman. Caco-2 monolayers in experimental and theoretical predictions of drug transport. *Adv. Drug Deliv. Rev* **46**:27–43 (2001).
52. A. Fasano, G. Budillon, S. Guandalini, R. Cuomo, G. Parrilli, A. M. Cangiotti, M. Morroni, and A. Rubino. Bile acids reversible effects on small intestinal permeability. An *in vitro* study in the rabbit. *Dig. Dis. Sci* **35**:801–808 (1990).
53. R. Moore, S. Carlson, and J. L. Madara. Rapid barrier restitution in an *in vitro* model of intestinal epithelial injury. *Lab. Invest* **60**:237–244 (1989).
54. K. Masuda, H. Ikeda, K. Kasai, Y. Fukuzawa, H. Nishimaki, T. Takeo, and G. Itoh. Diversity of restitution after deoxycholic acid-induced small intestinal mucosal injury in the rat. *Dig. Dis. Sci* **48**:2108–2115 (2003).
55. R. A. Argenizo, C. K. Henrikson, and J. A. Lisacos. Restitution of barrier and transport function of porcine colon after acute mucosal injury. *Am. J. Physiol* **255**:G62–G71 (1988).
56. J. A. Matovelo, T. Landsverk, and R. B. Sund. Alterations of ultrastructure and of cytoplasmic filaments in remodeling rat jejunal epithelial cells during recovery from deoxycholate. *APMIS* **98**:887–895 (1990).
57. A. Jacinto, A. Martinez-Arias, and P. Martin. Mechanisms of epithelial fusion and repair. *Nat. Cell Biol* **3**:E117–E123 (2001).
58. A. U. Dignass. Mechanisms and modulation of intestinal epithelial repair. *Inflamm. Bowel Dis* **7**:68–77 (2001).
59. D. A. Waller, N. W. Thomas, and T. J. Self. Epithelial restitution in the large intestine of the rat following insult with bile salts. *Virchows Arch. A Pathol. Anat. Histopathol* **414**:77–81 (1988).
60. K. Nakanishi, M. Masada, and T. Nadai. Effect of pharmaceutical adjuvants on the rectal permeability of drugs III. Effect of repeated administration and recovery of the permeability. *Chem. Pharm. Bull* **31**:4161–4166 (1983).
61. R. Moore, S. Carlson, and J. L. Madara. Villus contraction aids repair of intestinal epithelium after injury. *Am. J. Physiol* **257**: G274–G283 (1989).
62. S. Feldman and M. Reinhard. Interaction of sodium alkyl sulfates with everted rat small intestinal membrane. *J. Pharm. Sci* **65**:1460–1462 (1976).
63. D. A. Whitmore, L. G. Brookes, and K. P. Wheeler. Relative effects of different surfactants on intestinal absorption and the release of proteins and phospholipids from the tissue. *J. Pharm. Pharmacol* **31**:277–283 (1979).
64. M. A. Hurni, A. B. Noach, M. C. Blom-Roosemalen, A. G. de Boer, J. F. Nagelkerke, and D. D. Breimer. Permeability enhancement in Caco-2 cell monolayers by sodium salicylate and sodium taurodihydrofusidate: assessment of effect-reversibility and imaging of trans-epithelial transport routes by confocal laser scanning microscopy. *J. Pharmacol. Exp. Ther* **267**:942–950 (1993).
65. A. J. Hudspeth. Establishment of tight junctions between epithelial cells. *Proc. Natl. Acad. Sci. U.S.A* **72**:2711–2713 (1975).
66. C. K. Henrikson, R. A. Argenzio, J. A. Liacos, and J. Khosla. Morphologic and functional effects of bile salt on the porcine colon during injury and repair. *Lab. Invest* **60**:72–87 (1989).
67. J. A. Matovel, R. B. Sund, and T. Landsverk. Morphological and functional recovery following exposure to deoxycholic acid. A study in the rat small intestine *in vivo*. *APMIS* **97**:798–810 (1989).
68. M. Riegler, R. Sedivy, W. Feil, G. Hamilton, B. Teleky, G. Bischof, E. Cosentini, T. Sogukoglu, R. Schiessel, and E. Wenzl. Laminin stimulates rapid epithelial restitution of rabbit duodenal mucosa *in vitro*. *Scand. J. Gastroenterol* **31**:1167–1175 (1996).